Reactive uptake of glyoxal by particulate matter

John Liggio
Centre for Atmospheric Chemistry and Chemistry Department, York University, Toronto, Ontario, Canada

Shao-Meng Li
Meteorological Service of Canada, Toronto, Ontario, Canada

Robert McLaren
Centre for Atmospheric Chemistry and Chemistry Department, York University, Toronto, Ontario, Canada

Received 9 June 2004; revised 30 September 2004; accepted 17 December 2004; published 19 May 2005.

[1] The uptake of gaseous glyoxal onto particulate matter has been studied in laboratory experiments under conditions relevant to the ambient atmosphere using an aerosol mass spectrometer. The growth rates and reactive uptake coefficients, γ, were derived by fitting a model of particle growth to the experimental data. Organic growth rates varied from 1.05×10^{-11} to 23.1×10^{-11} μg particle^{-1} min^{-1} in the presence of $\sim$5 ppb glyoxal. Uptake coefficients (γ) of glyoxal varied from 8.0×10^{-4} to 7.3×10^{-3} with a median $\gamma = 2.9 \times 10^{-3}$, observed for $(NH_4)_2SO_4$ seed aerosols at 55% relative humidity. Increased γ values were related to increased particle acidity, indicating that acid catalysis played a role in the heterogeneous mechanism. Experiments conducted at very low relative humidity, with the potential to be highly acidic, resulted in very low reactive uptake. These uptake coefficients indicated that the heterogeneous loss of glyoxal in the atmosphere is at least as important as gas phase loss mechanisms, including photolysis and reaction with hydroxyl radicals. Glyoxal lifetime due to heterogeneous reactions under typical ambient conditions was estimated to be $\tau_{het} = 5-287$ min. In rural and remote areas the glyoxal uptake can lead to 5–257 ng m^{-3} of secondary organic aerosols in 8 hours, consistent with recent ambient measurements.

Citation: Liggio, J., S.-M. Li, and R. McLaren (2005), Reactive uptake of glyoxal by particulate matter, *J. Geophys. Res.*, *110*, D10304, doi:10.1029/2004JD005113.

1. Introduction

[2] Secondary organic aerosol (SOA) formation via gas-particle partitioning processes is an area of increased study. An understanding of these processes is important because aerosols play a role in climate change [*Pilinis et al.*, 1995; *Twomey*, 1991], visibility [*Eldering and Cass*, 1996; *Eldering et al.*, 1993; *Yuan et al.*, 2000], and adverse health effects [*Dockery et al.*, 1993; *Schwartz and Dockery*, 1992]. Significant progress has been made with respect to particulate organic product identification [*Bowman et al.*, 1997; *Pankow*, 1994a, 1994b]; however much of the studies has focused on low-volatility products, which are expected to easily partition into the particle phase on the basis of gas-particle partitioning theory. Recently studies have shown that volatile compounds can also be taken up by aerosols, particularly carbonyls known to be capable of heterogeneous reactions [*Jang et al.*, 2002, 2003; *Jang and Kamens*, 2001a; *Kalberer et al.*, 2004; *Noziere and Riemer*, 2003; *Olson and Hoffmann*, 1989; *Tobias and Ziemann*, 2000]. Although the role of gas phase carbonyls as a source of radicals [*Seinfeld and Pandis*, 1998] and organic nitrates [*Grosjean et al.*, 1996] has been studied extensively, little is known regarding their contribution to SOA by means of heterogeneous reactions. Potential mechanisms for this include hydration of the carbonyl followed by acid catalyzed polymerization or acetal/hemiacetal formation in the presence of alcohols [*Jang et al.*, 2002, 2003; *Jang and Kamens*, 2001a], aldol condensation reactions [*Noziere and Riemer*, 2003] as well as other reactions known to occur in bulk solution [*Olson and Hoffmann*, 1989; *Tobias and Ziemann*, 2000]. Evidence of the formation of organic sulfate compounds as a means of carbonyl uptake has also recently been presented [*Liggio et al.*, 2005]. Heterogeneous reactions of these types imply that SOA yields may be significantly larger than those predicted by partitioning theory, which is especially relevant given that most organic photo-oxidation products contain carbonyl functionality.

[3] Glyoxal is one of most prevalent dicarbonyls in the ambient atmosphere. It is primarily formed from the photo-oxidation of aromatic hydrocarbons [*Jang and Kamens*, 2001b; *Yu et al.*, 1997], and is also a minor oxidation product of isoprene [*Carter and Atkinson*, 1996; *Yu et al.*, 1995], and other biogenic species [*Fick et al.*, 2003]. The often high concentrations of aromatic and biogenic species in ambient air imply that partitioning of glyoxal could be a

0148-0227/05/2004JD005113$09.00

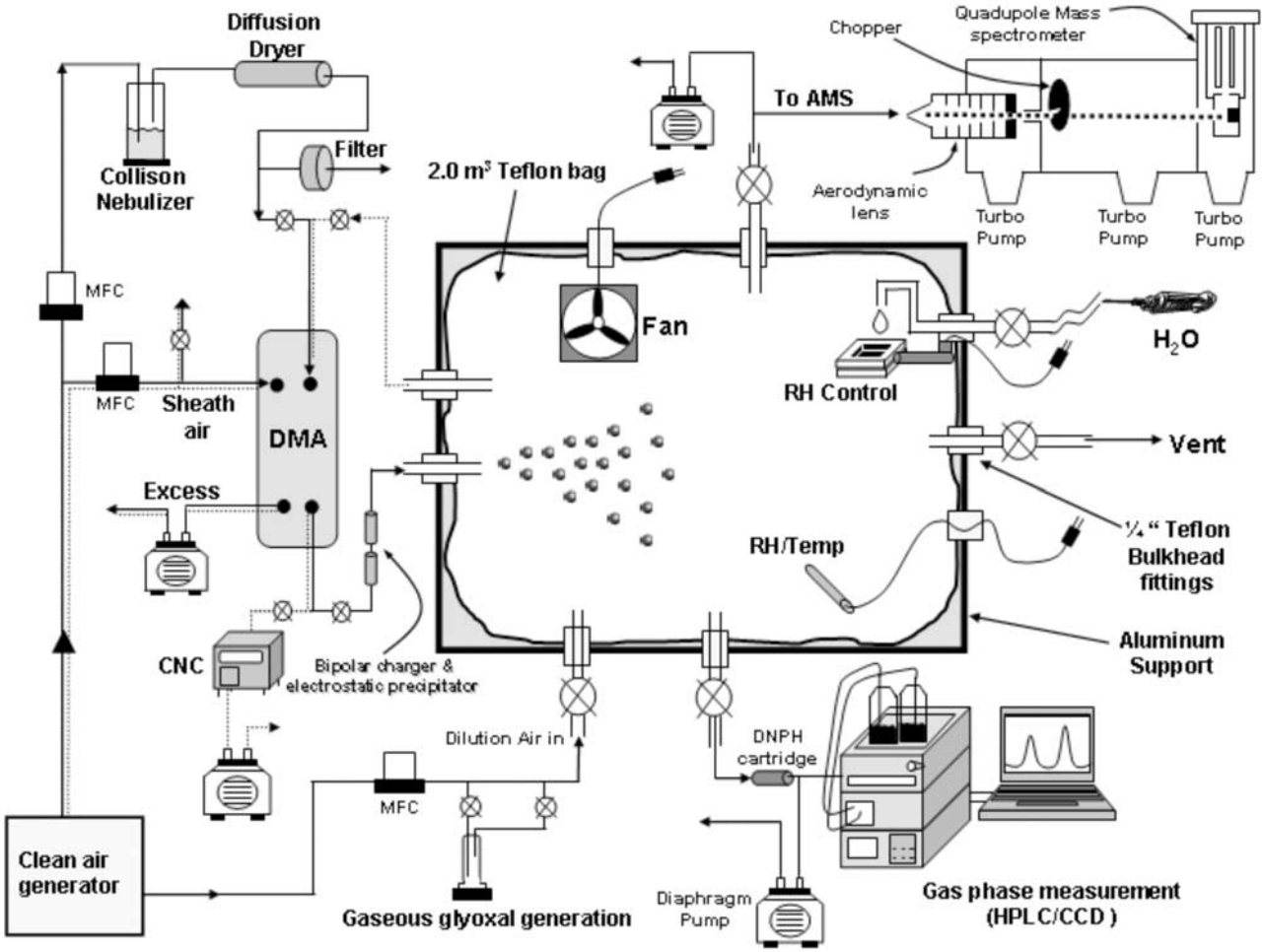

Figure 1. Schematic representation of experimental system. Dotted lines represent DMA/CNC sampling mode of operation. Solid lines represent the filling mode of operation.

significant contributor to SOA. In fact, glyoxal has been found to produce significant aerosol yields, attributed to hydration and polymerization [*Jang and Kamens*, 2001a]. Although the body of qualitative structural evidence is increasing for the formation of low-volatility products, a quantitative understanding of the significance of these reactions to the ambient atmosphere is lacking. Typically laboratory studies of these processes that have identified product compounds are performed under conditions significantly different than those of the ambient atmosphere. The elevated gas phase and particle concentrations associated with such experiments make a simple extrapolation to the ambient conditions difficult. More rigorous kinetic experiments have also been performed, primarily involving the reactive uptake of carbonyl species such as formaldehyde and acetone on aqueous droplets, sulfuric acid films or bulk solution [*Duncan et al.*, 1999; *Iraci and Tolbert*, 1997; *Jayne et al.*, 1996; *Tolbert et al.*, 1993]. The kinetics for the reactive uptake of glyoxal onto particles more closely simulating ambient material would be a useful tool in an assessment of the atmospheric importance of this process. In a previous paper [*Liggio et al.*, 2005] a heterogeneous mechanism for this uptake as well as mass spectral evidence for the formation of glyoxal-acetals and sulfates has been presented.

[4] In the present work, a simple uptake model is fit to the experimental data obtained during the study on reactive uptake of glyoxal [*Liggio et al.*, 2005] to determine the reactive uptake coefficient (γ). This coefficient is defined as the probability that a collision between a gas molecule and the particle surface will result in uptake, considering all aspects of the uptake process including diffusion, mass accommodation, solubility and reactivity. Data were obtained by exposing seed aerosols to gas phase glyoxal within a chamber while an aerosol mass spectrometer (AMS) was used to probe the chemical composition of the growing particles and quantify the total organic content. Particle mass spectra were obtained on line during reactive uptake. The effect of seed composition, in particular particle acidity and relative humidity, on the observed uptake coefficients and growth rates will be presented. The atmospheric implications of this uptake will also be discussed.

2. Experimental Description

[5] The entire apparatus utilized in these experiments is given schematically in Figure 1. A detailed description of this system has been reported previously [*Liggio et al.*, 2005]. Briefly, studies were conducted in a 2 m^3 Teflon

Table 1. Summary of the Initial Conditions and Particle Growth During Uptake Experiments

Experiment	Nebulizer Solution,[a] M	RH, %	Gaseous Glyoxal, ppb	Initial Diameter,[b] nm	Final Diameter, nm
1	$SO_4^{2-} = 0.024$ $NH_4^+ = 0.048$ $H_3O^+ = 5 \times 10^{-6}$	49	5.1	127.8	339.1
2	$SO_4^{2-} = 0.024$ $NH_4^+ = 0.048$ $H_3O^+ = 5 \times 10^{-6}$	98	4.9	201.7	409.1
3	$HSO_{4-} = 0.033$ $SO_4^{2-} = 0.029$ $H_3O^+ = 0.042$ $NH_4^+ = 0.048$	55	4.8	248.1	507.5
4	$HSO_{4-} = 0.033$ $SO_4^{2-} = 0.029$ $H_3O^+ = 0.042$ $NH_4^+ = 0.048$	98	3.6	258.1	478.1
5	$HSO_{4-} = 0.033$ $SO_4^{2-} = 0.029$ $H_3O^+ = 0.042$ $NH_4^+ = 0.048$	11	4.9	232.7	232.7
6	$HSO_4^- = 0.096$ $SO_4^{2-} = 0.042$ $H_3O^+ = 0.130$ $NH_4^+ = 0.050$	50	4.5	289.4	522.6
7	$HSO_4^- = 0.096$ $SO_4^{2-} = 0.042$ $H_3O^+ = 0.130$ $NH_4^+ = 0.050$	88	5.3	231.7	440.1
8	$NaCl = 4.63 \times 10^{-3}$ $KCl = 1.14 \times 10^{-3}$ $MgCl_2 = 7.5 \times 10^{-3}$ $CaCl_2 = 1.1 \times 10^{-3}$	70	4.9	248.1	478.1
9	$NaNO_3 = 0.038$	60	5.4	271.4	426.4
10	$NO_{3-} = 0.060$ $Na^+ = 0.038$ $H_3O^+ = 0.022$	65	5.1	272.4	414.4

[a]Equilibrium concentrations are presented. Experiments 1and 2 particles are produced from $(NH_4)_2SO_4$ solution, experiments 3–7 from $(NH_4)_2SO_4$ acidified with varying amounts of H_2SO_4, and experiment 10 from $NaNO_3$ solution acidified with HNO_3.
[b]Initial diameter refers to the aerodynamic diameter after initial hygroscopic growth, if any, measured by the AMS.

bag (Whelch Flurocarbon Inc.) enclosed in an aluminum support. Particles of known inorganic composition were introduced into the bag with pre-existing gaseous glyoxal. Particle growth was determined with a scanning differential mobility analyzer (DMA) and condensation nuclei counter (CNC) as well as an aerosol mass spectrometer (AMS, Aerodyne Research Inc.). Mass spectra of particles were obtained with the AMS to provide the structural and size information for the organic mass.

[6] Monodisperse particles were generated by atomizing aqueous solutions of different chemical composition with a Collison Nebulizer (BGI Inc.) followed by sizing with the DMA. A complete list of the solutions used and other experimental conditions is given in Table 1. The effect of particle acidity and relative humidity (RH) on the uptake of glyoxal was studied by increasing the H_2SO_4 concentration in an $(NH_4)_2SO_4$ nebulizer solution and by varying the RH from 11 to 98% in the chamber.

[7] Gaseous glyoxal was produced by dehydration of the commercially available solid glyoxal trimeric dihydrate (Aldrich) as described elsewhere [*Steacie et al.*, 1935]. This yielded gas phase monomeric glyoxal, which was flushed directly into the chamber via a stream of clean air. Glyoxal concentrations remained approximately constant during the course of single experiments between 3.6 and 5.4 ppbv. Gaseous glyoxal measurements were made using an automated version of a 2,4-DNPH cartridge method coupled to HPLC system equipped with a variable wavelength UV absorbance detector [*Aiello*, 2003].

[8] The composition and size of the particles were monitored with the AMS over the course of each experiment (1.5–4 hours). Numerous publications have described the operation and applications of the AMS [*Allan et al.*, 2003a, 2003b; *Jayne et al.*, 2000; *Jimenez et al.*, 2003]. In brief, particles are sampled through a critical orifice and aerodynamic lens system, which focuses the particles into a narrow beam and accelerates them into the time of flight region. A chopper is present which may either completely block the particle beam or allow some material through at a defined frequency. The velocity and hence size of the particle can be calculated from the time taken to reach a heated surface from the chopper. Particles are then impacted on the heated surface where they are vaporized and subsequently ionized by electron impact (EI) and carried into a quadrupole mass spectrometer for mass analysis.

3. Results and Discussion

[9] A summary of the extent of particle growth for all experiments is given in Table 1. Generally particle growth was significant for most experiments regardless of the seed particle composition. Various inorganic particles were utilized, including ammonium sulfate (experiments 1 and 2), ammonium sulfate acidified with sulfuric acid to varying degrees (experiments 3–7), sea salt (experiment 8), sodium nitrate (experiment 9) and sodium nitrate acidified with nitric acid (experiment 10). In most cases, particles approximately doubled in diameter during the course of each experiment except experiment 5, which was conducted at very low relative humidity. The net organic mass uptake by the particles varied from 4.8 to 46 $\mu g\ m^{-3}$. The net increases are significantly more than can be accounted for by glyoxal solubility based solely on Henry's law. The concentration of a species in the aqueous fraction of particles based on Henry's law can be given as

$$C_p = HC_g(MW)W\left(1 \times 10^{-3}\right), \quad (1)$$

where C_p is the particulate phase concentration of the species of interest ($\mu g\ m^{-3}$), H the effective Henry's law constant ($M\ atm^{-1}$), C_g the gas phase concentration (atm), MW the molecular weight ($g\ mol^{-1}$) and W the available particle water content ($\mu g\ m^{-3}$). If the Kelvin effect of the particle curvature is considered, C_p will be reduced from that predicted by equation (1). For a typical example relevant to this study, W was estimated at 5 $\mu g\ m^{-3}$ or approximately 20% of a total particle mass of 25 $\mu g\ m^{-3}$. Substitution of this and other known parameters (C_g = 5 ppb, MW = 58 $g\ mol^{-1}$, $H = 3.6 \times 10^5$ $M\ atm^{-1}$) into equation (1) results in a C_p of approximately 5.3×10^{-4} $\mu g\ m^{-3}$. Thus, although the effective Henry's law constant for glyoxal is rather large [*Zhou and Mopper*, 1990a], only a minor fraction would be present in the aqueous phase based solely on hydration.

[10] As the calculated value based on hydration is several orders of magnitude smaller than what is observed experimentally, further reaction of the hydrated glyoxal must have taken place. A mechanism for this reaction is presented

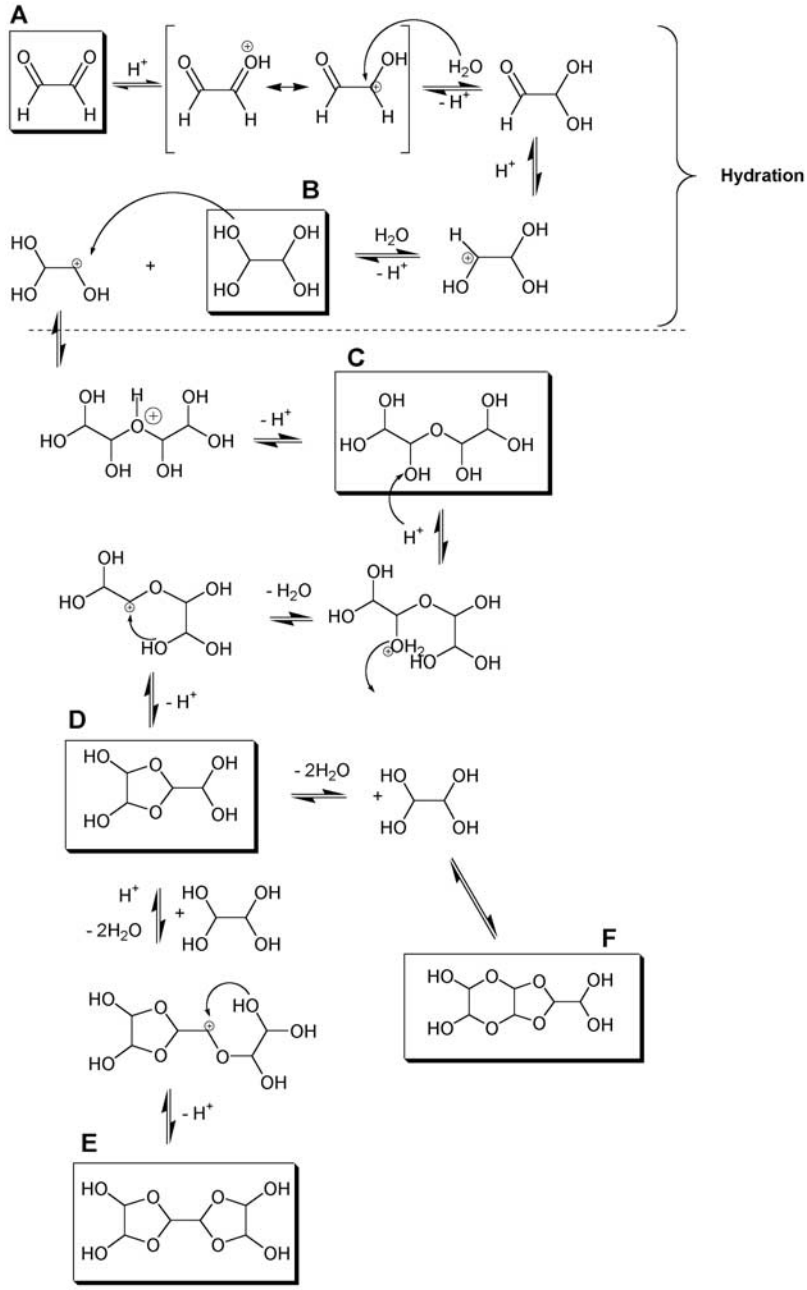

Figure 2. Mechanism for the uptake and subsequent reaction of glyoxal in particulate matter.

in Figure 2, which has been postulated in a previous paper [*Liggio et al.*, 2005], involving hydration and subsequent cyclic acetal formation of compounds containing up to 3 monomer units. Larger oligomers may arise over a longer period of time. These acetal ring structures have been identified in the AMS mass spectra for the particles [*Liggio et al.*, 2005]. However, a quantitative assessment of the relative importance of each oligomer, from the overall particle mass spectra, is not possible. This is primarily because many fragments can arise from several or all observed products, and reference spectra for these compounds are unavailable.

[11] A common difficulty associated with chamber experiments is the particle wall losses. Because of the losses, decreases in the measured organic mass over time are not necessarily indicative of reductions in the reactive uptake. To remove the effect of particle wall losses on the observed organic growth, the ratio of organic mass to sulfate mass in the particles was determined and is given in Figure 3. This ratio is proportional to the organic mass on a per particle basis since the mass of SO_4^{2-} per particle does not change over time. Particle SO_4^{2-} was measured on the AMS simultaneously with the organic mass, among others, and in fact this is one of the intrinsic advantages of using the AMS for this study.

[12] Although a doubling of diameter (Table 1) indicated that particles took up significant amounts of organic material, the full extent of glyoxal reactive uptake is only observed in Figure 3. After 1 hour, the ratio of organic to sulfate mass was approximately 2 for many experiments,

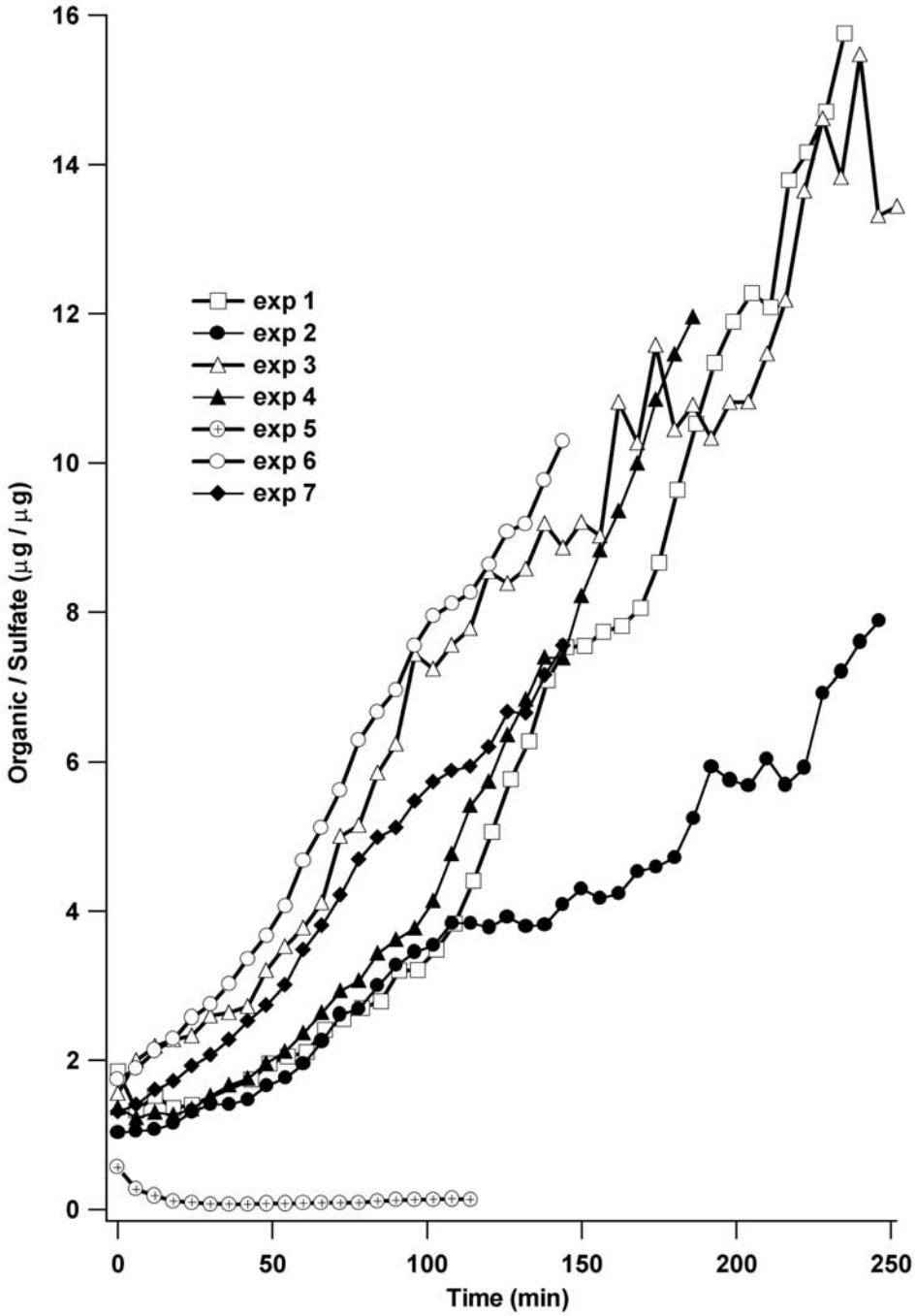

Figure 3. Ratio of organic mass to sulfate mass as a function of time for selected experiments, as determined by the AMS.

but after 4 hours the ratio increased to greater than 10 for several experiments, indicating that the particles became primarily organic in nature. Also, the growth curves presented in Figure 3 tend to show an accelerated growth at longer times as indicated by the slightly positive curvatures. These growth rates on a per particle basis are given in Table 2. The organic mass per particle is determined by multiplying the ratio in Figure 3 by the constant SO_4^{2-} per particle which is derived from the AMS sulfate mass and the particle number distributions. The growth rate per particle at any given time is the slope of the curve at that time, or the numerical derivative of a fit to the uptake model described below. Accordingly the organic growth rates varied by experiment between 1.0×10^{-11} and 2.7×10^{-10} μg particle^{-1} min^{-1}, and during the course of a single experiment were accelerated by up to 54%. The observed acceleration in the rate of uptake is likely a result of the increasing surface area available as the particles grow, as discussed further below. Also shown in Table 2 are the average growth rates in the geometric diameter of the particles determined from the DMA data (nm min^{-1}). Growth rates of the particles determined from the DMA

Table 2. Total Organic Growth Rates and Uptake Coefficients

Experiment[a]	Seed Type	RH, %	Particle pH[b]	Mean Diameter Growth Rate,[c] nm min^{-1}	Mass Growth Rate Range,[d] $\mu g\ particle^{-1}\ min^{-1} \times 10^{11}$	Mean Mass Growth Rate,[d] $\mu g\ particle^{-1}\ min^{-1} \times 10^{11}$	γ
1	$(NH_4)_2SO_4$	49	<6	0.37	5.3–6.8	6.0	2.6×10^{-3}
2	$(NH_4)_2SO_4$	98	6	0.37	4.3–5.7	5.0	2.2×10^{-3}
3	$(NH_4)_2SO_4/H_2SO_4$	55	−0.73	0.33	11.3–15.0	13.1	2.9×10^{-3}
4	$(NH_4)_2SO_4/H_2SO_4$	98	−0.48	0.90	13.4–20.7	16.9	7.3×10^{-3}
5	$(NH_4)_2SO_4/H_2SO_4$	11	−1.3	0.10	1.03–1.1	1.05	8.0×10^{-4}
6	$(NH_4)_2SO_4/H_2SO_4$	50	−0.91	0.63	17.3–22.4	19.8	5.0×10^{-3}
7	$(NH_4)_2SO_4/H_2SO_4$	88	−0.44	0.83	20.3–26.1	23.1	4.8×10^{-3}
9	$NaNO_3$	60	7	1.3	8.1–8.8	8.5	2.3×10^{-3}
10	$NaNO_3/HNO_3$	65	−0.71	1.0	19.1–26.1	22.5	6.6×10^{-3}

[a]Growth rates and uptake coefficients for experiment 8 are indeterminable because of the inability of the AMS to quantify the seed mass (~NaCl) under the current experimental conditions.
[b]Particle pH is approximate value calculated with the Aerosol Inorganic model (AIM). Particle pH for experiment 1 could not be calculated with the AIM model because of formation of solids in the model. Assuming that a very small fraction of water exists, the pH of this fraction is likely less than that of experiment 2.
[c]Numbers are determined from DMA data, using mean initial and final geometric diameters.
[d]Numbers are determined from AMS data, using mean of the dynamic growth rates.

geometric diameters, and presuming a density of 1.3 g cm^{-3}, compare favorably to the organic growth rates determined from the AMS data.

3.1. Uptake Model

[13] A measure of the reactive uptake of glyoxal including all inherent chemical reactions as a whole can be determined in the form of an uptake coefficient (γ). On the basis of kinetic theory of gasses, the net rate of transfer (Φ_{net}) of gas molecules in and out of a given particle can be derived by considering the gas collision rate with a stationary surface, and the particle surface area. It can be expressed as

$$\Phi_{net} = \Phi_{in} - \Phi_{out} = \gamma \pi a^2 \langle c \rangle \left(C_\infty - C_{eq}\right), \tag{2}$$

where γ is the uptake coefficient, a the particle radius and $\langle c \rangle$ the mean molecular speed of the gas given by $(8RT/\pi MW)^{1/2}$. C_∞ and C_{eq} represent the gas phase concentration far away, and in equilibrium with the particle surface, respectively. The overall second-order rate of reaction can then be expressed as Φ_{net} multiplied by the particle number density (N_p) or

$$\frac{dC_{org}}{dt} = \gamma \pi a^2 \langle c \rangle C_g N_p = k_R C_g N_p, \tag{3}$$

where the rate of gas phase loss is equal to the rate of change of the particulate organic concentration (C_{org}). C_g is the gas phase concentration derived by assuming that $C_{eq} \ll C_\infty$. The rate of change of organic mass on a per particle basis, m_{org}, is obtained by dividing equation (3) by N_P, and incorporating a heterogeneous mass factor, F_h, that accounts for the increase in organic mass as it reacts heterogeneously from the reactant (glyoxal) to form particulate phase organic material. The nature of this mass factor will be discussed later. Hence

$$\frac{dm_{org}}{dt} = \gamma \pi a^2 \langle c \rangle C_g F_h. \tag{4}$$

In these experiments the organic mass loading ($\mu g_{org}\ m^{-3}$) is measured as a function of time with the AMS, from which the organic mass per particle is calculated. The uptake coefficient is determined by fitting the experimental data to a theoretical model, also describing the increase in organic mass per particle (m_{org}). In the current simple model a spherical inorganic particle with initial radius a_o and volume V_o is exposed to gas phase glyoxal and grows to a radius of a and volume V (Figure 4). For this analysis it is assumed that the uptake is irreversible and that the aerosol is monodisperse. The difference in volume (growth) can be related to the additional organic mass added, through the density of the organic mass by

$$\left(\frac{4}{3}\pi a^3 - \frac{4}{3}\pi a_o^3\right)\rho = m_{org}, \tag{5}$$

where ρ is the density of the organic mass. Rearrangement of equation (5) gives a relationship between the radius of the particle and the added organic mass given by

$$a = \left(\frac{3m_{org}}{4\pi\rho} + a_o^3\right)^{\frac{1}{3}}, \tag{6}$$

which is substituted into equation (4) to yield a differential equation where only m_{org} is time dependent,

$$\int_{m_0}^{m} \left(b m_{org} + d\right)^{-2/3} dm_{org} = \int_{t_0}^{t} k\, dt, \tag{7}$$

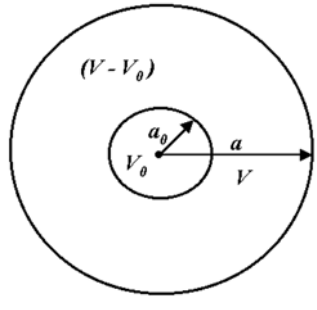

Figure 4. Schematic of the uptake model.

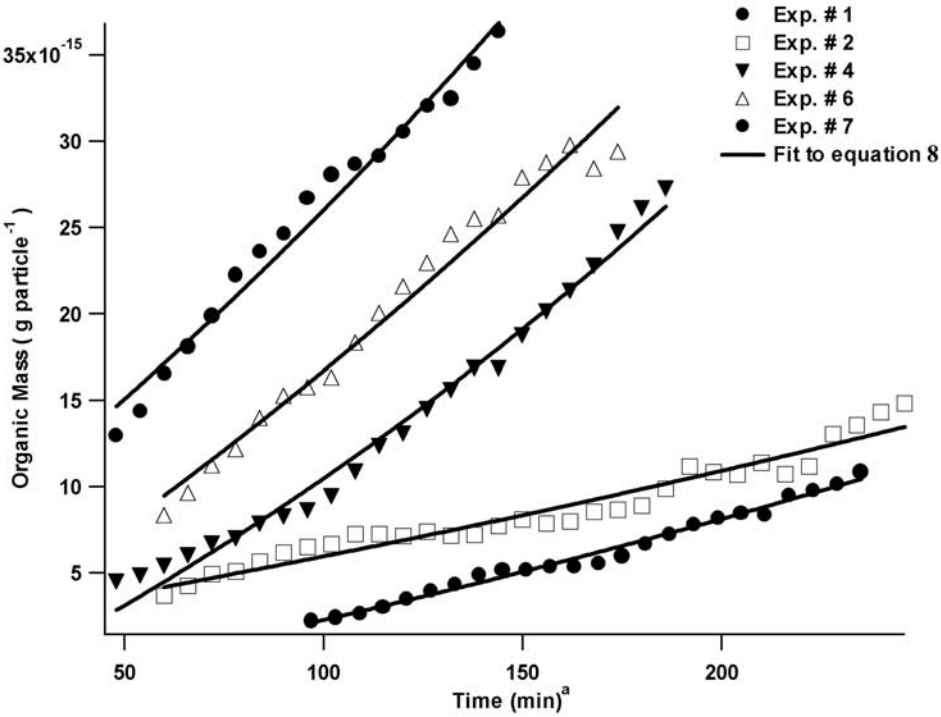

Figure 5. Organic mass per particle as a function of time fit to equation (8) for selected experiments.

where

$$k = \gamma\pi C_g\langle c\rangle F_k \qquad b = \frac{3}{4\pi\rho} \qquad d = a_0^3.$$

Since particles were introduced into the chamber over a prolonged period of time, some particles must have experienced more growth than others during the filling process. Consequently the limits of integration were chosen so as to only include data collected after the particle filling period was complete. Therefore the left side of equation (7) was integrated from the mass at the end of filling (m_0) to mass m, and the right side integrated from the end of the filling period (t_0) to some time t. The constants m_0 and t_0 were taken directly from the experimental data. Integration of equation (7) with the above limits yields a relation for the organic mass as a function of time,

$$m_{org} = \left(\frac{bk(t-t_0) + 3(bm_0 + d)^{1/3}}{3b^{1/3}}\right)^3 - \frac{d}{b}. \qquad (8)$$

3.2. Determination of γ

[14] A plot of m_{org} as a function of time for selected experiments is presented in Figure 5. Equation (8) is fit to this experimental data and is also presented in Figure 5. The uptake coefficients are obtained from the parameter k where C_g and $\langle c\rangle$ are known. The heterogeneous mass factor, F_h, was chosen using the following reasoning. A change in mass occurs for the specific case of a heterogeneous reaction of glyoxal, by incorporation of 2 water molecules into the molecular formula of the final organic product through the hydration reactions (Figure 2). The organic mass measured by the AMS includes the additional mass of these water molecules. In this case F_h is larger than 1.0 and can be obtained by taking the ratio of the molecular weight of the final product $(C_2H_2O_2)_n(H_2O)_2$ n = 1, 2, 3; to the molecular weight of n units of glyoxal monomer: $n(C_2H_2O_2)$ n = 1, 2, 3. The corresponding values of the heterogeneous correction factors, F_h (n) would be: 1.62 (n = 1), 1.31 (n = 2) and 1.21 (n = 3). The value n = 1 corresponds to the formation of the gemdiol in solution (B in Figure 2), which has previously been argued to be a minor component of the mix, as is likely the case for product C. In this study, since we cannot determine the relative proportions of the different products (B, C, D, E, F), we have used a value of $F_h = 1.26$, the average value for n = 2 (product D) and n = 3 (product E), for the determination of the reactive uptake coefficients. The formation of higher oligomers (n > 3) is possible, although the value of F_h only drops to 1.10 (n = 6). The best fit for these experiments was obtained by fixing the constants b and d, with the density of the organic mass estimated as 1.3 g cm^{-3} and the initial seed radius (a_o) determined experimentally from the mean of the size distribution. The error associated with the correction factor is expected to be considerably smaller than the uncertainties related to the organic mass determination via the AMS. These include uncertainties with respect to the particle focusing efficiency of the AMS for ammonium sulfate, and the ionization efficiency of the organic mass in the absence of an authentic reference standard. These uncertainties are likely significantly larger than the uncertainty in the chosen value of F_h which is expected to be less than 10%. The relative uncertainty in the k parameter derived from the fitting procedure (from which γ is calculated) ranged from 1.8 to 10%. The gas phase glyoxal measurement has an estimated

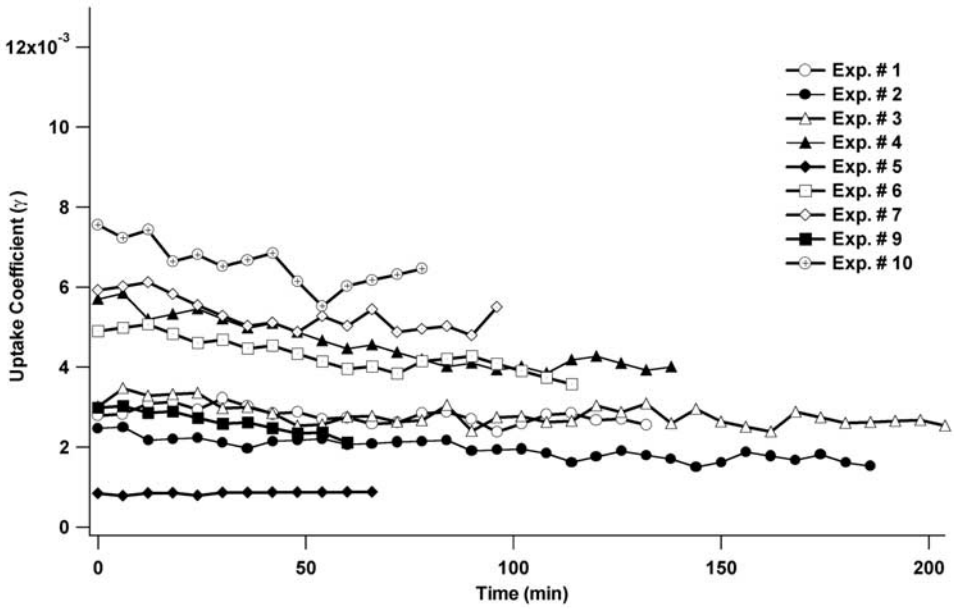

Figure 6. Uptake coefficients determined by differentiation of equation (8) as a function of time.

accuracy of 20%, which likely contributes most significantly to the overall uncertainty of the uptake coefficients. A conservative estimate of the overall uncertainty in the calculated uptake coefficients is approximately 40%. Uptake coefficients derived in this manner including the above corrections are presented in Table 2.

[15] An alternative approach in calculating the uptake coefficients is to fit the experimental data to equation (8), substitute the fit parameters back into this equation, and numerically differentiate the result. The result is the analytical expression

$$\frac{dm_{org}}{dt} = 3bk\left(\frac{bk(t-t_0)+3(bm_0+d)^{1/3}}{3b^{1/3}}\right)^2. \qquad (9)$$

The numerical value for this relation at a given time is set equal to equation (4), from which substitution of the experimental particle radius at each time step, and other constants from equation (4) gives the uptake coefficient as a function of time. The results of this approach are presented in Figure 6 for several experiments and verify that the uptake coefficient is roughly constant over time. The uptake coefficient calculated by this approach and averaged over time, is in good agreement with those calculated directly from the fit. The relative standard deviation between the calculation methods ranged from 0.83 to 8.1%.

[16] A slight decrease in γ over time can be observed for some experiments. This decrease is statistically significant in some cases, and is in the range of -10% to -15% per hour. One might expect a decrease in γ over time since the particles transform from primarily inorganic to organic composition over the course of the experiment. The relatively small change in γ during this transformation likely indicates that the uptake is largely determined by the presence of water. This argument would be consistent with the proposed first step of the heterogeneous reaction, solvation. The similarity of the absolute values of γ, and those measured in water (37), also supports this argument.

[17] Calculated uptake coefficients (Table 2) varied from 8.0×10^{-4} to 7.3×10^{-3}, and are in general agreement with uptake coefficients determined for glyoxal on aqueous droplets ($\gamma \sim 10^{-3}$) using a droplet train technique [*Schweitzer et al.*, 1998]. No other data are available regarding the uptake of glyoxal. However, the range of observed γ is also consistent with those for other carbonyl compounds reported in literature, on a variety of substrates. The formaldehyde/sulfuric acid system has been the most common system studied to date, with uptake coefficients measured on sulfuric acid films ($\gamma \sim 2 \times 10^{-3}$) [*Iraci and Tolbert*, 1997], droplets ($\gamma = 2.7 \times 10^{-3} - 2.7 \times 10^{-2}$) [*Jayne et al.*, 1996], and bulk solution ($\gamma = 1 \times 10^{-2} - 8 \times 10^{-2}$) [*Tolbert et al.*, 1993]. Uptake coefficients for other carbonyls including acetaldehyde, acetone and propionaldehyde, on mineral oxide particles have also been reported ($\gamma \sim 10^{-4} - 10^{-6}$) [*Li et al.*, 2001] and are significantly lower. Not only are uptake coefficients in this work in reasonable agreement with γ of similar systems, but also consistent with the presumption in the literature that heterogeneous reactions must occur to result in the observed uptake parameters.

3.3. Effect of Acidity and Humidity

[18] The approximate pH of the particles has been calculated using an aerosol inorganic model (AIM) [*Clegg et al.*, 1998]. Given that initial molar ratios and RH conditions were used as input into the model, the resultant pH values likely only represent particles at the beginning of experiments, and do not take into account changes in the hygroscopicity or organic content as the particles grow. However, modeled pH values do serve as a relative measure of the acidity of particles between experiments. The results of the present work indicate that the reactive uptake of glyoxal may be acid catalyzed in some instances. In general, γ increased by a factor of $\sim$2–3 when an

acidified seed was used compared to nonacidified seeds under similar conditions (Table 2: experiments 1 versus 6, experiments 2 versus 4 or 7, and experiments 9 versus 10). This implies that the nature of the acid is likely unimportant as only acidic protons are necessary, consistent with the proposed heterogeneous reaction mechanism. The effect of particle acidity is also evident in the particle growth rates presented in Table 2 and the organic to seed ratios in Figure 3. Experiments using non acidified $(NH_4)_2SO_4$ particles (experiments 1 and 2) exhibited growth rates of $5 - 6 \times 10^{-11}$ μg particle^{-1} min^{-1}, compared to $13.1 - 23.1 \times 10^{-11}$ μg particle^{-1} min^{-1} for acidified seed particles. A similar effect is observed for acidified and nonacidified $NaNO_3$ particles (8.5×10^{-11} and 22.5×10^{-11} μg particle^{-1} min^{-1}, respectively). Recent publications have also suggested that reactive uptake of carbonyls is likely acid catalyzed [*Jang et al.*, 2003; *Jang and Kamens*, 2001a].

[19] Although the presence of acid increases the rate of heterogeneous reaction, acidic aerosols were not necessary for the uptake to occur, and even with a decrease of 8 pH units, uptake coefficients and growth rates increased at most by a factor of only 3. Significant growth was observed on nonacidified $(NH_4)_2SO_4$, NaCl and $NaNO_3$ particles (experiments 1, 2, and 9) with reasonably high growth rates and uptake coefficients. This is consistent with uptake efficiencies for glyoxal on aqueous droplets, which have been shown to have negligible pH dependence at temperatures approaching room temperature [*Schweitzer et al.*, 1998] and with recent studies which found that polymerization in aerosols does not require acid catalysis [*Kalberer et al.*, 2004].

[20] Other deviations from an acid catalyzed model have also been noted in this study. Growth rates and uptake coefficients for experiments 4 and 7 (pH −0.48 and −0.44) are unexpectedly larger or similar to those for experiments 3 and 6 (pH −0.73 and −0.91) even though less acidic particles were utilized. This may be a result of potentially unstable reaction products under highly acidic conditions, whose decomposition may compete with formation reactions. Studies of the depolymerization of glyoxal dimers has shown that a reverse process is in fact acid catalyzed with a rate constant that increases substantially in solutions with a pH below 2 [*Fratzke and Reilly*, 1986]. Slightly less acidic particles may also promote the formation of some more prevalent oligomers while reducing the rate of formation for others.

[21] Experiments at low relative humidities are expected to produce particles with low pH, and thus potentially result in significant reactive uptake in an acid catalyzed model. However the reactive uptake of glyoxal for such an experiment (RH 11%, experiment 5) was significantly less than all other experiments resulting in no significant increase in particle diameter. The resultant uptake coefficient (8.0×10^{-4}) and growth rate (1.05×10^{-11} μg particle^{-1} min^{-}1) were also considerably less than all others. In addition, the particles produced during the experiment contained an organic fraction that constituted less than 10% of the total particle mass. This may be explained by noting that at very low RH, sufficiently below the deliquescence point, the aqueous content of the particles as well as the amount of hydrated glyoxal is likely very small. As a result, fast heterogeneous reactions can potentially deplete the available aqueous layer and completely consume the gem-diol precursors. Without the necessary precursors, further reactive uptake of glyoxal is halted as observed in Figure 3. Reestablishment of an aqueous equilibrium with the particles would result in the additional uptake of water and glyoxal, which in turn would allow the heterogeneous reactions to continue. However, it is likely that the initial reactive uptake producing a somewhat hydrophobic mass significantly changed the hygroscopic nature of the particles, thus preventing further water uptake from occurring. This may have implications for reactive uptake of glyoxal on ambient urban particles that are primarily hydrophobic.

[22] The effect of particle acidity is also evident in the time evolution of many of the mass fragments observed in particle mass spectra. The evolution of several of these ions normalized to a SO_4^{2-} fragment ion (m/z 48) is given in Figure 7. Normalization removes the effect of particle wall losses and results in a signal that is proportional to the concentration of the species associated with a given fragment on a per particle basis. With the exception of experiment 5, the evolution of fragments (m/z 117 and 135) known to arise predominantly from glyoxal oligomers [*Liggio et al.*, 2005], was slowed upon RH increases and hence pH. This effect in Figure 7 is most prevalent, when comparing sets of experiments with the same initial particle composition but conducted at different RH (experiments 1 versus 2, experiments 3 versus 4, and experiments 6 versus 7). Since the time evolution of oligomer fragments is proportional to the oligomerization rate, a delay in this rate may also be an indication of acid catalysis given that dilution at higher RH reduces the particle acidity. Conversely, dilution may reduce the concentration of the gem-diol precursor, and hence also slow the rate of oligomerization. This is only possible where gas phase diffusion of glyoxal to the particle surface is a rate-limiting step in the overall process, since gas-particle equilibrium would require the hydrated glyoxal concentration to remain constant.

[23] Which of the above scenarios is operating depends upon the likelihood that gas phase diffusion of glyoxal is rate limiting. This can be evaluated by determining whether these experiments were performed in the diffusion or gas kinetic limit. According to the add-as resistance model [*Molina et al.*, 1996], the condition for a diffusion limited process is that $3a/\lambda \gg 4/\alpha$, where a represents the particle radius, λ the gas mean free path and α the mass accommodation coefficient. The mean free path (λ) is given by $3D_G/\langle c \rangle$ where D_G is the diffusion constant for glyoxal in air, estimated as 0.3 cm^2 s^{-1}, intermediate to D_G in $H_2O_{(g)}$ and He which have been calculated elsewhere [*Schweitzer et al.*, 1998]. The mean free path is calculated to be approximately 2.73×10^{-7} m and an accommodation coefficient (α) of 0.023 for glyoxal on aqueous droplets [*Schweitzer et al.*, 1998] is assumed to be similar to that in the present experiments. Substitution of these parameters as well as a typical particle radius of 230 nm into the above inequality results in $3a/\lambda = 2.5$ and $4/\alpha = 173.9$. Consequently, the process occurring here is likely not diffusion limited, as extremely large particles are required in this system to satisfy the above inequality. Therefore it is more likely that a reduction in particle acidity caused by an increase in the

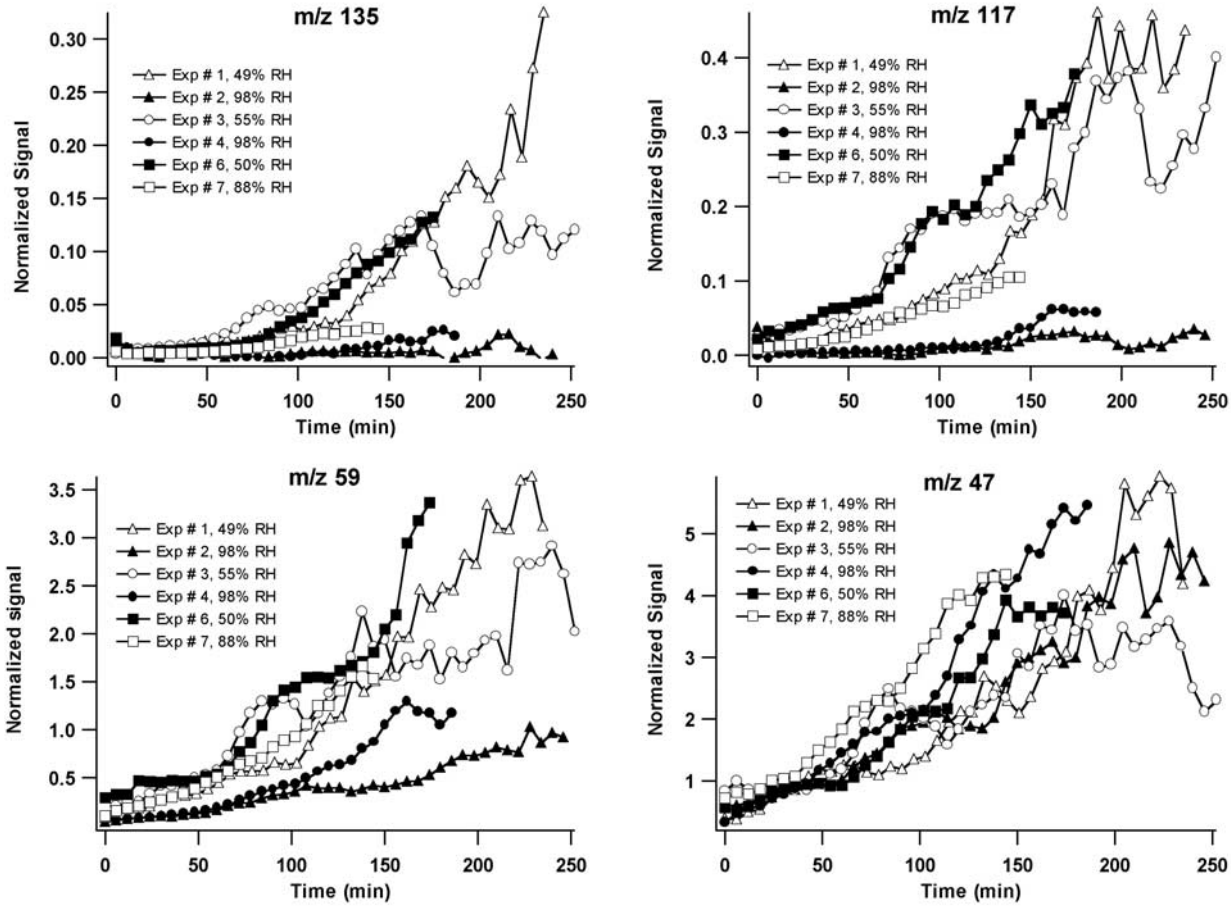

Figure 7. Time evolution of selected ions from experiments 1, 2, 3, 4, 6, and 7. Organic ion signals are normalized to the SO_4^{2-} signal (m/z 48) to remove the effect of particle wall losses on fragment evolution.

RH produced the observed decline of the fragment evolution and oligomerization rate.

[24] However, an acid catalysis effect in Figure 7 (experiment 1 versus experiment 2, experiment 3 versus experiment 4, and experiment 6 versus experiment 7) for a fragment thought to arise primarily from the hydrated glyoxal (m/z 47), is not clear. In this case an increase in RH has either the opposite or no effect on the fragment evolution. This is an indication that the formation of hydrated glyoxal is more dependent on the aqueous content than the particle acidity. In addition, the fragment evolution for masses that can potentially arise from several oligomers or the hydrated monomer (m/z 59 – Figure 7) is not slowed as significantly upon increasing the RH. Consequently, it is likely that several different oligomers are formed, some by reactions that are more subject to acid catalysis than others. As a result, the magnitude of the reactive uptake of glyoxal may not differ tremendously between highly acidic and nonacidic particles, while the relative contribution of each oligomer may differ significantly.

3.4. Atmospheric Implications

[25] Given that several of these experiments were performed under conditions similar to the real atmosphere (a low initial aerosol seed mass loading, 50% relative humidity and ppbv levels of glyoxal), it is reasonable to expect these reactions to occur in ambient aerosols as a means of uptake of glyoxal and other carbonyls. The range of particle acidities utilized in these experiments was also consistent with pH of ambient aerosols, which have been measured as low as −2.4 [*Li et al.*, 1997]. Currently, direct evidence of a polymerization reaction for glyoxal in ambient aerosols has not been confirmed on the basis of structural identification of products. Indirectly, however, extraction and DNPH derivatization of ambient particulate material has revealed such a process likely occurred (J. Liggio and R. McLaren, Observations of volatile secondary organic carbonyls in atmospheric particulates, manuscript in preparation, 2005, hereinafter referred to as Liggio and McLaren, manuscript in preparation, 2005). During the extraction procedure mild heating caused polymeric structures to revert to monomeric starting material (glyoxal). The DNPH derivatization also served to shift equilibrium toward the free form of glyoxal. Detection of this free glyoxal can explain the higher than expected levels found in ambient particulate matter [*Liggio and McLaren*, 2003]. The extremely slow kinetics associated with the extraction and derivatization of ambient material also indicated that a thermal decomposition of some polymer likely occurred. This is principally because

Table 3. Estimation of Heterogeneous Glyoxal Reaction Rate Constants and Associated Lifetime Compared With Known Gaseous Loss Processes

Environment	Surface Area,[a] μm^2 cm^3	Parameter k,[b] s^{-1}	τ_{het},[c] min
Rural	7.9×10^2	1.9×10^{-4}	89
Remote	1.1×10^3	2.7×10^{-4}	61
Free troposphere	2.4×10^2	5.8×10^{-5}	287
Urban	1.4×10^4	3.4×10^{-3}	5
Reaction with OH[d]		5.5×10^{-5}	300
Photolysis[e]		7.88×10^{-5}	211
Total gas phase loss[f]		1.34×10^{-4}	125

[a]Area is adapted from typical surface area distributions (18).
[b]Parameter k is given as pseudo first order.
[c]Lifetime is given as the inverse of first-order rate constant.
[d]In this case, it is assumed that [OH] = 5×10^6 molecules cm^{-3} and $k_{OH} = 1.1 \times 10^{-11}$ cm^3 $molecules^{-1}$ s^{-1} [*Atkinson et al.*, 1989].
[e]Numbers are j value for midday maximum [*Jenkin et al.*, 1996].
[f]Total is the sum of photolysis and OH reaction rate constants.

an extraction time on the order of days had been necessary for ambient aerosol samples, as compared to an hour for the derivatization of aqueous glyoxal in bulk solution or adsorbed to the surface of a sampling filter. Aspects of these experiments are described elsewhere (Liggio and McLaren, manuscript in preparation, 2005).

[26] The derived uptake coefficients can be used to perform simple calculations as an estimate of the significance of glyoxal uptake to ambient particulate matter. The importance of this uptake as a gas phase glyoxal removal process is evaluated against other gas phase loss mechanisms by comparing the associated lifetimes. Results of this analysis are presented in Table 3. Pseudo first-order rate constants for the heterogeneous reaction of glyoxal are determined by substitution of the appropriate parameters into the relation for the rate constant given in equation (3). This constant is given by $k = \frac{1}{4} \gamma \langle c \rangle S$, where S is the total particle surface area (μm^2 cm^{-3}). Typical total particle surface areas for several environments were adapted from the appropriate model surface distributions [*Seinfeld and Pandis*, 1998]. A reactive uptake coefficient of 2.9×10^{-3}, corresponding to the median value of the experiments, and more similar to the coefficients obtained at reasonable ambient RH (55%) was used in this evaluation. The estimated pseudo first-order rate constants span 2 orders of magnitude ($5.8 \times 10^{-5} - 3.4 \times 10^{-3}$ s^{-1}) depending on the environment, and hence the heterogeneous lifetime (τ_H), given by the inverse of the rate constant also varies significantly (5–287 min). The heterogeneous lifetimes determined here for rural, remote, and free tropospheric conditions are somewhat shorter than the individual lifetimes for glyoxal due to photolysis or OH radical reaction, but more similar to the overall gas phase lifetime given in Table 3. The heterogeneous lifetime under urban conditions however, is significantly shorter than the overall gas phase glyoxal lifetime. These results indicate that even under relatively clean conditions, heterogeneous glyoxal loss rates are comparable to loss rates due to other gas phase processes, and are significantly faster in more polluted regions. If the heterogeneous reactions are irreversible as implied in these experiments, then a net decrease in the production of HO_x from glyoxal and potentially many other carbonyl compounds may result. Given that formaldehyde has been estimated to contribute 25–30% of the total radical production at midday [*Lee et al.*, 1998], and glyoxal 10–15% [*Aiello*, 2003], the heterogeneous loss to particle of these aldehydes implies that this reduction in HO_x may be significant.

[27] The uptake of glyoxal may also be a significant source of secondary organic particulate matter. To emphasize this possibility, the rate of formation of particulate organic mass resulting from the reactive uptake of glyoxal was estimated, and is presented in Table 4. The rates were calculated from the pseudo first-order rate constants in Table 3 and typical gas phase glyoxal measurements for those areas [*Cerqueira et al.*, 2003; *Destaillats et al.*, 2002; *Grosjean et al.*, 2002; *Grossmann et al.*, 2003; *Kleinman et al.*, 1994; *Lee et al.*, 1995, 1998; *Spaulding et al.*, 2002, 2003; *Zhou and Mopper*, 1990b]. The results of the calculations show that formation rates vary appreciably ($1.4 \times 10^{-6} - 8.0 \times 10^{-4}$ μg $m^{-3} s^{-1}$) with location, and that large amounts of organic mass can be produced in a short time. Under rural, remote and free tropospheric conditions 5–250 ng m^{-3} of particulate phase glyoxal can be produced in eight hours, while urban conditions can produce an organic mass that exceeds that in other areas by up to an order of magnitude (2.9–23.0 μg m^{-3}). Such a large organic mass associated with one compound in urban

Table 4. Estimation of Ambient Organic Mass That Can Be Formed From Reactive Uptake of Glyoxal

Environment	Gaseous Glyoxal [ ],[a] ppb	Organic Mass Formation Rate,[b] μg m^{-3} s^{-1}	Potential Organic Mass Produced, μg m^{-3}		
			1 hour	2 hours	8 hours
Rural	0.02	8.92×10^{-6}	0.032	0.064	0.257
Remote	0.01	6.50×10^{-6}	0.023	0.047	0.187
Free troposphere	0.01	1.38×10^{-6}	0.005	0.010	0.040
Urban	0.1	7.98×10^{-4}	2.87	5.74	22.97

[a]Numbers are typical measured values.
[b]Rate is calculated as k (Figure 5) × [glyoxal].

areas is unlikely. However, the true uptake coefficient for urban particles is likely considerably less if a significant fraction of those aerosols contain soot or other nonhygroscopic mass as evidenced by the reduced uptake of experiment 5. In addition, the gas phase glyoxal concentration in an urban plume may decrease dramatically as it is transported away from a source. Hence the rate of glyoxal uptake will also decrease sharply over the same eight hour period, reducing the above urban estimate. Estimates for other atmospheric conditions are not unreasonable for a single compound, and the few measurements of ambient particulate glyoxal that exist are somewhat consistent with the estimates provided here.

[28] Particulate glyoxal has been measured in rural/biogenic areas to be as low as 1–5 ng m^{-3} [*Liggio and McLaren*, 2003] and as high as 150 ng m^{-3} [*Matsunaga et al.*, 2003]. Particulate glyoxal in marine ($\sim$1.8 ng m^{-3}) and polar environments (0.003–2.29 ng m^{-3}) has also been measured [*Kawamura*, 1993; *Kawamura et al.*, 1996]. To date, only a single urban measurement of particulate glyoxal appears in the literature [*Kawamura*, 1993]. This measurement, from approximately 30 km west of Tokyo, at a level of 46 ng m^{-3} is significantly less than the above estimates for urban areas. Given the numerous carbonyl species present in the atmosphere and the many possible heterogeneous reactions, uptake of carbonyls to aerosols may be a significant contributor to SOA and demands further study.

[29] **Acknowledgments.** We would like to acknowledge the National Science and Engineering Research Council and the Meteorological Service of Canada for funding. We thank Kathy Hayden and Richard Leaitch for their technical expertise in operation of the AMS. We thank Michael Mozurkewich and Tak Wai Chan for use of, and technical support with, the DMA/CNC system.

References

Aiello, M. (2003), An automated instrument for the quantitation of atmospheric carbonyls: Measurements and interpretation in southern Ontario, Ph.D. thesis, York Univ., Toronto, Ont., Canada.

Allan, J. D., et al. (2003a), Quantitative sampling using an Aerodyne aerosol mass spectrometer: 2. Measurements of fine particulate chemical composition in two U.K. cities, *J. Geophys. Res.*, *108*(D3), 4091, doi:10.1029/2002JD002359.

Allan, J. D., J. L. Jimenez, P. I. Williams, M. R. Alfarra, K. N. Bower, J. T. Jayne, H. Coe, and D. R. Worsnop (2003b), Quantitative sampling using an Aerodyne aerosol mass spectrometer: 1. Techniques of data interpretation and error analysis, *J. Geophys. Res.*, *108*(D3), 4090, doi:10.1029/2002JD002358.

Atkinson, R., D. L. Baulch, R. A. Cox, R. F. Hampson Jr., J. A. Kerr, and J. Troe (1989), Evaluated kinetic and photochemical data for atmospheric chemistry, *J. Phys. Chem. Ref. Data Suppl. III*, *18*(2), 881–1097.

Bowman, F. M., J. R. Odum, J. H. Seinfeld, and S. Pandis (1997), Mathematical model for gas-particle partitioning of secondary organic aerosols, *Atmos. Environ.*, *31*, 3921–3931.

Carter, W. P. L., and R. Atkinson (1996), Development and evaluation of a detailed mechanism for the atmospheric reactions of isoprene and NO_x, *Int. J. Chem. Kinet.*, *28*(7), 497–530.

Cerqueira, M. A., C. A. Pio, P. A. Gomes, J. S. Matos, and T. V. Nunes (2003), Volatile organic compounds in rural atmospheres of central Portugal, *Sci. Total Environ.*, *313*(1–3), 49–60.

Clegg, S. L., P. Brimblecombe, and A. S. Wexler (1998), A thermodynamic model of the system H-NH4-Na-SO_4-NO_3-Cl-H_2O at 298.15 K, *J. Phys. Chem. A*, *102*, 2155–2171.

Destaillats, H., R. S. Spaulding, and M. J. Charles (2002), Ambient air measurement of acrolein and other carbonyls at the Oakland–San Francisco Bay Bridge toll plaza, *Environ. Sci. Technol.*, *36*(10), 2227–2235.

Dockery, D. W., C. A. Pope III, X. Xu, J. D. Spengler, J. H. Ware, M. E. Fay, B. G. Ferris Jr., and F. E. Speizer (1993), An association between air pollution and mortality in six U.S. cities, *N Engl. J. Med.*, *329*(24), 1753–1759.

Duncan, J. L., L. R. Schindler, and J. T. Roberts (1999), Chemistry at and near the surface of liquid sulfuric acid: A kinetic, thermodynamic, and mechanistic analysis of heterogeneous reactions of acetone, *J. Phys. Chem. B*, *103*, 7247–7259.

Eldering, A., and G. R. Cass (1996), Source-oriented model for air pollutant effects on visibility, *J. Geophys. Res.*, *101*(D14), 19,343–19,369.

Eldering, A., S. M. Larson, J. R. Hall, K. J. Hussey, and G. R. Cass (1993), Development of an improved image processing based visibility model, *Environ. Sci. Technol.*, *27*(4), 626–635.

Fick, J., L. Pommer, C. Nilsson, and B. Andersson (2003), Effect of OH radicals, relative humidity, and time on the composition of the products formed in the ozonolysis of a-pinene, *Atmos. Environ.*, *37*, 4087–4096.

Fratzke, A. R., and P. J. Reilly (1986), Thermodynamic and kinetic analysis of the dimerization of aqueous glyoxal, *Int. J. Chem. Kinet.*, *18*(7), 775–789.

Grosjean, D., E. Grosjean, and L. F. R. Moreira (2002), Speciated ambient carbonyls in Rio de Janeiro, Brazil, *Environ. Sci. Technol.*, *36*(7), 1389–1395.

Grosjean, E., D. Grosjean, and J. H. Seinfeld (1996), Atmospheric chemistry of 1-octene, 1-decene, and cyclohexene: Gas-phase carbonyl and reroxyacyl nitrate products, *Environ. Sci. Technol.*, *30*(3), 1038–1047.

Grossmann, D., et al. (2003), Hydrogen peroxide, organic peroxides, carbonyl compounds, and organic acids measured at Pabstthum during BERLIOZ, *J. Geophys. Res.*, *108*(D4), 8250, doi:10.1029/2001JD001096.

Iraci, L. T., and M. A. Tolbert (1997), Heterogeneous interaction of formaldehyde with cold sulfuric acid: Implications for the upper troposphere and lower stratosphere, *J. Geophys. Res.*, *102*(D13), 16,099–16,107.

Jang, M., and R. M. Kamens (2001a), Atmospheric secondary aerosol formation by heterogeneous reactions of aldehydes in the presence of a sulfuric acid aerosol catalyst, *Environ. Sci. Technol.*, *35*(24), 4758–4766.

Jang, M., and R. M. Kamens (2001b), Characterization of secondary aerosol from the photooxidation of toluene in the presence of NO_x and 1-propene, *Environ. Sci. Technol.*, *35*(18), 3626–3639.

Jang, M., N. M. Czoschke, S. Lee, and R. M. Kamens (2002), Heterogeneous atmospheric aerosol production by acid-catalyzed particle-phase reactions, *Science*, *298*(5594), 814–817.

Jang, M., B. Carroll, B. Chandramouli, and M. K. Richard (2003), Particle growth by acid-catalyzed heterogeneous reactions of organic carbonyls on preexisting aerosols, *Environ. Sci. Technol.*, *37*(17), 3828–3837.

Jayne, J. T., D. R. Worsnop, C. E. Kolb, E. Swartz, and P. Davidovits (1996), Uptake of gas-phase formaldehyde by aqueous acid surfaces, *J. Phys. Chem.*, *100*, 8015–8022.

Jayne, J. T., D. C. Leard, X. Zhang, P. Davidovits, K. A. Smith, C. E. Kolb, and D. R. Worsnop (2000), Development of an aerosol mass spectrometer for size and composition analysis of submicron particles, *Aerosol Sci. Technol.*, *33*(1–2), 49–70.

Jenkin, M. E., S. M. Saunders, and M. J. Pilling (1996), The tropospheric degradation of volatile organic compounds: A protocol for mechanism development, *Atmos. Environ.*, *31*, 81–104.

Jimenez, J. L., et al. (2003), Ambient aerosol sampling using the Aerodyne Aerosol Mass Spectrometer, *J. Geophys. Res.*, *108*(D7), 8425, doi:10.1029/2001JD001213.

Kalberer, M., et al. (2004), Identification of polymers as major components of atmospheric organic aerosols, *Science*, *303*(5664), 1659–1662.

Kawamura, K. (1993), Identification of C_2-C_3 ω-oxocarboxylic acids, pyruvic acid, and C_2-C_3 α-dicarbonyls in wet precipitation and aerosol samples by capillary GC and GC/MS, *Anal. Chem.*, *65*(23), 3505–3511.

Kawamura, K., H. Kasukabe, and L. A. Barrie (1996), Source and reaction pathways of dicarboxylic acids, ketoacids and dicarbonyls in arctic aerosols: One year of observations, *Atmos. Environ.*, *30*, 1709–1722.

Kleinman, L., et al. (1994), Ozone formation at a rural site in the southeastern United States, *J. Geophys. Res.*, *99*(D2), 3469–3482.

Lee, Y.-N., X. Zhou, and K. Hallock (1995), Atmospheric carbonyl compounds at a rural southeastern United States site, *J. Geophys. Res.*, *100*(D12), 25,933–25,944.

Lee, Y.-N., et al. (1998), Atmospheric chemistry and distribution of formaldehyde and several multioxygenated carbonyl compounds during the 1995 Nashville/Middle Tennessee Ozone Study, *J. Geophys. Res.*, *103*(D17), 22,449–22,462.

Li, P., K. A. Perreau, E. Covington, C. H. Song, G. R. Carmichael, and V. H. Grassian (2001), Heterogeneous reactions of volatile organic compounds on oxide particles of the most abundant crustal elements: Surface reactions of acetaldehyde, acetone, and propionaldehyde on SiO_2, Al_2O_3, Fe_2O_3, TiO2, and CaO, *J. Geophys. Res.*, *106*(D6), 5517–5529.

Li, S.-M., A. M. Macdonald, J. W. Strapp, Y. N. Lee, and X. L. Zhou (1997), Chemical and physical characterizations of atmospheric aerosols over southern California, *J. Geophys. Res.*, *102*(D17), 21,341–21,353.

Liggio, J., and R. McLaren (2003), An optimized method for the determination of volatile and semi-volatile aldehydes and ketones in ambient particulate matter, *Int. J. Environ. Anal. Chem.*, *83*(10), 819–835.

Liggio, J., S.-M. Li, and R. McLaren (2005), Heterogeneous reactions of glyoxal on particulate matter: Identification of acetals and sulfate esters, *Environ. Sci. Technol.*, *39*(6), 1532–1541.

Matsunaga, S., M. Mochida, A. Guenntther, R. Schnell, J. Greenberg, K. Kawamura, and Y. Kajii (2003), A measurement of gaseous and particulate biogenic semi-volatile organic compounds in the forest atmosphere with an annular denuder sampling system, *Eos Trans. AGU*, *84*(46), Fall Meet. Suppl., Abstract A32A-0113.

Molina, M. J., L. T. Molina, and C. E. Kolb (1996), Gas-phase and heterogeneous chemical kinetics of the troposphere and stratosphere, *Annu. Rev. Phys. Chem.*, *47*, 327–367.

Noziere, B., and D. D. Riemer (2003), The chemical processing of gas-phase carbonyl compounds by sulfuric acid aerosols: 2,4-pentandione, *Atmos. Environ.*, *37*, 841–851.

Olson, T. M., and M. R. Hoffmann (1989), Hydroxyalkylsulfonate formation: Its role as a sulfur(IV) reservoir in atmospheric water droplets, *Atmos. Environ.*, *23*, 985–997.

Pankow, J. F. (1994a), An absorption model of the gas/aerosol partitioning involved in the formation of secondary organic aerosol, *Atmos. Environ.*, *28*, 189–193.

Pankow, J. F. (1994b), An absorption model of gas/particle partitioning of organic compounds in the atmosphere, *Atmos. Environ.*, *28*, 185–188.

Pilinis, C., S. N. Pandis, and J. H. Seinfeld (1995), Sensitivity of direct climate forcing by atmospheric aerosols to aerosol size and composition, *J. Geophys. Res.*, *100*(D9), 18,739–18,754.

Schwartz, J., and D. W. Dockery (1992), Particulate air pollution and daily mortality in Steubenville, Ohio, *Am. J. Epidemiol.*, *135*(1), 12–19.

Schweitzer, F., L. Magi, P. Mirabel, and C. George (1998), Uptake rate measurements of methanesulfonic acid and glyoxal by aqueous droplets, *J. Phys. Chem. A*, *102*, 593–600.

Seinfeld, J. H., and S. Pandis (1998), *Atmospheric Chemistry and Physics: From Air Pollution to Climate Change*, John Wiley, Hoboken, N. J.

Spaulding, R. S., R. W. Talbot, and M. J. Charles (2002), Optimization of a mist chamber (cofer scrubber) for sampling water-soluble organics in air, *Environ. Sci. Technol.*, *36*(8), 1798–1808.

Spaulding, R. S., G. W. Schade, A. H. Goldstein, and M. J. Charles (2003), Characterization of secondary atmospheric photooxidation products: Evidence for biogenic and anthropogenic sources, *J. Geophys. Res.*, *108*(D8), 4247, doi:10.1029/2002JD002478.

Steacie, E. W. R., W. H. Hatcher, and J. F. Horwood (1935), Kinetics of the decomposition of gaseous glyoxal, *J. Chem. Phys.*, *3*, 291–295.

Tobias, H. J., and P. J. Ziemann (2000), Thermal desorption mass spectrometric analysis of organic aerosol formed from reactions of 1-tetradecene and O_3 in the presence of alcohols and carboxylic acids, *Environ. Sci. Technol.*, *34*(11), 2105–2115.

Tolbert, M. A., J. Pfaff, I. Jayaweera, and M. J. Prather (1993), Uptake of formaldehyde by sulfuric acid solutions: Impact on stratospheric ozone, *J. Geophys. Res.*, *98*(D2), 2957–2962.

Twomey, S. (1991), Aerosols, clouds and radiation, *Atmos. Environ., Part A*, *25*, 2435–2442.

Yu, J., H. E. Jeffries, and R. M. Le Lacheur (1995), Identifying airborne carbonyl compounds in isoprene atmospheric photooxidation products by their PFBHA oximes using gas chromatography/ion trap mass spectrometry, *Environ. Sci. Technol.*, *29*(8), 1923–1932.

Yu, J., H. E. Jeffries, and K. G. Sexton (1997), Atmospheric photooxidation of alkylbenzenes: I. Carbonyl product analyses, *Atmos. Environ.*, *31*, 2261–2280.

Yuan, C. S., C. G. Lee, J. C. Chang, S. H. Liu, C. Yuan, and H. Y. Yang (2000), Correlation of atmospheric visibility with chemical composition and size distribution of aerosol particles in urban area, paper presented at 93rd Air and Waste Management Association Annual Conference and Exhibition, Salt Lake City, Utah.

Zhou, X., and K. Mopper (1990a), Apparent partition coefficients of 15 carbonyl compounds between air and seawater and between air and freshwater: Implications for air-sea exchange, *Environ. Sci. Technol.*, *24*(12), 1864–1869.

Zhou, X., and K. Mopper (1990b), Measurement of sub-parts-per-billion levels of carbonyl compounds in marine air by a simple cartridge trapping procedure followed by liquid chromatography, *Environ. Sci. Technol.*, *24*(10), 1482–1485.

S.-M. Li, Meteorological Service of Canada, 4905 Dufferin Street, Toronto, ON, Canada M3H 5T4.

J. Liggio and R. McLaren, Centre for Atmospheric Chemistry and Chemistry Department, York University, 4700 Keele Street, Toronto, ON, Canada M3J 1P3. (rmclaren@yorku.ca)